PNNL-17480

0099756

Pacific Northwest National Laboratory
Operated by Battelle for the U.S. Department of Energy

Challenges Associated with Apatite Remediation of Uranium in the 300 Area Aquifer

DM Wellman
JS Fruchter
VR Vermeul
MD Williams

RECEIVED
OCT 17 2011
EDMC

April 2008

Prepared for the U.S. Department of Energy
under Contract DE-AC05-76RL01830

attached to: 0099752

DISCLAIMER

This report was prepared as an account of work sponsored by an agency of the United States Government. Neither the United States Government nor any agency thereof, nor Battelle Memorial Institute, nor any of their employees, makes **any warranty, express or implied, or assumes any legal liability or responsibility for the accuracy, completeness, or usefulness of any information, apparatus, product, or process disclosed, or represents that its use would not infringe privately owned rights**. Reference herein to any specific commercial product, process, or service by trade name, trademark, manufacturer, or otherwise does not necessarily constitute or imply its endorsement, recommendation, or favoring by the United States Government or any agency thereof, or Battelle Memorial Institute. The views and opinions of authors expressed herein do not necessarily state or reflect those of the United States Government or any agency thereof.

PACIFIC NORTHWEST NATIONAL LABORATORY
operated by
BATTELLE
for the
UNITED STATES DEPARTMENT OF ENERGY
under Contract DE-AC05-76RL01830

Printed in the United States of America

Available to DOE and DOE contractors from the
Office of Scientific and Technical Information,
P.O. Box 62, Oak Ridge, TN 37831-0062;
ph: (865) 576-8401
fax: (865) 576-5728
email: reports@adonis.osti.gov

Available to the public from the National Technical Information Service,
U.S. Department of Commerce, 5285 Port Royal Rd., Springfield, VA 22161
ph: (800) 553-6847
fax: (703) 605-6900
email: orders@ntis.fedworld.gov
online ordering: http://www.ntis.gov/ordering.htm

This document was printed on recycled paper.
(9/2003)

PNNL-17480

Challenges Associated with Apatite Remediation of Uranium in the 300 Area Aquifer

DM Wellman
JS Fruchter
VR Vermeul
MD Williams

April 2008

Prepared for
the U.S. Department of Energy
under Contract DE-AC05-76RL01830

Pacific Northwest National Laboratory
Richland, Washington 99352

Executive Summary

For fiscal year 2006, the United States Congress authorized $10 million dollars to Hanford for "...analyzing contaminant migration to the Columbia River, and for the introduction of new technology approaches to solving contamination migration issues." These funds are administered through the U.S. Department of Energy Office of Environmental Management (specifically, EM-22). After a peer review and selection process, nine projects were selected to meet the objectives of the appropriation. As part of this effort, Pacific Northwest National Laboratory (PNNL) is performing bench- and field-scale treatability testing designed to evaluate the efficacy of using polyphosphate injections to reduce uranium concentrations in the groundwater to meet drinking water standards (30 μg/L) in situ. This technology works by forming phosphate minerals (autunite and apatite) in the aquifer, which directly sequesters the existing aqueous uranium in autunite minerals and precipitates apatite minerals for sorption and long-term treatment of uranium migrating into the treatment zone, thus reducing current and future aqueous uranium concentrations. Polyphosphate injection was selected for testing based on technology screening as part of the 300-FF-5 Phase III Feasibility Study for treatment of uranium in the 300 Area.

The objective of the treatability test was to evaluate the efficacy of using polyphosphate injections to treat uranium-contaminated groundwater in situ. A test site consisting of an injection well and 15 monitoring wells was installed in the 300 Area near the process trenches that had previously received uranium-bearing effluents. This report summarizes the issues limiting the formation of apatite within the test. Two separate overarching issues impact the efficacy of apatite remediation for uranium sequestration within the 300 Area: 1) the efficacy of apatite for sequestering uranium under the present geochemical and hydrodynamic conditions, and 2) the formation and emplacement of apatite via polyphosphate technology.

Acronyms and Abbreviations

BTC	breakthrough curve
$CaCl_2$	calcium-chloride
K_d	equilibrium distribution coefficient
LFI	limited field investigation
R_{ef}	effective retardation

Contents

Executive Summary iii
Acronyms and Abbreviations iv
1.0 Introduction 1.1
2.0 Effect of 300 Area Hydrodynamic Conditions on Apatite Formation 2.1
2.1 High Flow Velocities 2.1
2.2 Low Surface Area 2.3
2.3 High Solution-to-Apatite Ratio 2.4
3.0 Effect of 300 Area Geochemical Conditions on the Removal and Long-Term Retention of Uranium with Apatite 3.1
3.1 Effects of pH on Adsorption of Uranium on Apatite 3.1
3.2 Effects of Speciation on the Sequestration of Uranium on Apatite 3.3
4.0 Summary 4.1
5.0 References 5.1

Figures

2.1 Polyphosphate Treatability Test Site Well Layout 2.2
2.2 Normalized BTC for Calcium, Phosphorus, Chloride, and Bromide at Down-Gradient Well 399-1-29 ..... 2.4
2.3 Uranium Loading on Hydroxyapatite 2.5
3.1 Historical pH Values of Selected Near-River and Inland Wells in the 300 Area 3.2
3.2 Dependence of Uranium Sequestration with Apatite Given a Solution-to-Solid Ratio of 325 mL/g Apatite 3.3
3.3 Dependence of Uranium Uptake Expressed as Aqueous Uranium Concentration as a Function of Time over the pH Range of 6 to 8 in Hydroxyapatite-Equilibrated Groundwater. ... 3.3
3.4 Equilibrium Distribution Coefficients for Uranium Sorption on Hydroxyapatite as a Function of pH 3.4
3.5 Percent Release of Uranyl from Hydroxyapatite as a Function of the Cumulative Volume of Hanford Groundwater. 3.5

Tables

2.1 Pilot-Scale Field Test Amendment Formulation 2.2
2.2 Transport Parameters Determined by Direct Measurement or from a Laboratory-Derived Breakthrough Curve on the <2-mm Sediment Fraction 2.3
2.3 Field Transport Parameters Calculated from Laboratory-Derived Transport Parameters 2.3
2.4 Bromide Tracer Injection Arrival Times and Porosity Results for Targeted Injection Volume Monitoring Wells 2.5

1.0 Introduction

Sequestration of uranium as insoluble phosphate phases appears to be a promising alternative for treating the uranium-contaminated groundwater at the Hanford 300 Area. The proposed approach involves both the direct formation of autunite by the application of a polyphosphate mixture, as well as the formation of apatite in the aquifer as a continuing source of phosphate for long-term treatment of uranium. After a series of bench-scale tests, a field treatability test was conducted in a well at the 300 Area. The objective of the treatability test was to evaluate the efficacy of using polyphosphate injections to treat uranium-contaminated groundwater in situ. A test site consisting of an injection well and 15 monitoring wells was installed in the 300 Area near the process trenches that had previously received uranium-bearing effluents. The results indicated that while the direct formation of autunite appears to have been successful, the outcome of the apatite formation of the test was more limited. Two separate overarching issues impact the efficacy of apatite remediation for uranium sequestration within the 300 Area: 1) the efficacy of apatite for sequestering uranium under the present geochemical and hydrodynamic conditions, and 2) the formation and emplacement of apatite via polyphosphate technology. This paper summarizes these issues.

2.0 Effect of 300 Area Hydrodynamic Conditions on Apatite Formation

Three hydrodynamic conditions affected the results of the treatability test: 1) the relatively high groundwater velocities that characterize the 300 Area unconfined aquifer, 2) the lack of surface area related to the large size of the clasts in the aquifer, and 3) the high solution-to-apatite ratios caused by limitations on the amount of apatite-forming reagents that could be introduced to the subsurface, coupled with rapid dispersal of the reagents.

2.1 High Flow Velocities

A tracer injection and drift test were conducted at the polyphosphate treatability test site (Figure 2.1) at the Hanford 300 Area on December 13, 2006. The test consisted of injecting 143,000 gal of tracer solution over an 11.9-hour period, then allowing the tracer plume to drift under natural gradient conditions toward a well located 31.7 m down gradient. The tracer drift duration was defined as the time period between the end of the injection period when the tracer plume was centered over the injection well (t = 714 minutes) and the arrival time of the center of mass at well 399-1-32 (t = ~3,700 minutes) (Figure 2.1). Based on results from this large-scale tracer test, groundwater velocity was estimated to be ~15 m/day. The time-weighted average gradient during tracer transport between the injection well and monitoring well 399-1-32, as determined from water-level measurements, was ~6.5E-4 m/m. Using these parameters, the estimated hydraulic conductivity is about 4,300 m/day which was consistent with property estimates obtained from analysis of hydraulic response data. However, the test results also suggest there are heterogeneities in the aquifer that could affect groundwater transport within, and down gradient, of the targeted treatment zone.

Based on the results of previous laboratory testing, a three-phase injection strategy was identified as an effective approach for achieving both direct treatment of the uranium contamination in groundwater (i.e., autunite formation) and secondary formation of calcium-phosphate phases (Table 2.1). The three-phase injection strategy consisted of an initial polyphosphate amendment injection to precipitate aqueous uranium as autunite, followed by an injection of a calcium-chloride ($CaCl_2$) solution to provide a sufficient calcium source for apatite formation during a subsequent polyphosphate injection. Because of the low solubility of calcium-phosphate phases, mixing calcium and phosphorus together prior to injection will result in the ex situ precipitation of calcium-phosphate phases. Thus, retardation and hydrodynamic dispersion of calcium and phosphate with the natural sedimentary matrix is critical to allow for the mixing of the sequential injections, which ultimately results in precipitation. The expectation was that the higher retardation of calcium would allow for mixing with the final polyphosphate injection, resulting in the formation of apatite.

Laboratory-scale column experiments were conducted to quantify the mobility of ortho-, pyro-, and tripolyphosphate, individually and as a mixed formulation (Table 2.1, injection 1) to evaluate differences in retardation due to interaction between the various phosphate compounds and to evaluate the mobility of calcium to determine the volume of reactants necessary to treat the desired zone. Saturated column tests were conducted with the <2-mm sediment fraction from 300 Area cores. The conditions and measured parameters for all of the transport experiments are summarized in Table 2.2. R is the retardation factor and K_d is the apparent distribution coefficient calculated from R. Transport experiments were conducted at a v of ~20 cm h^{-1}.

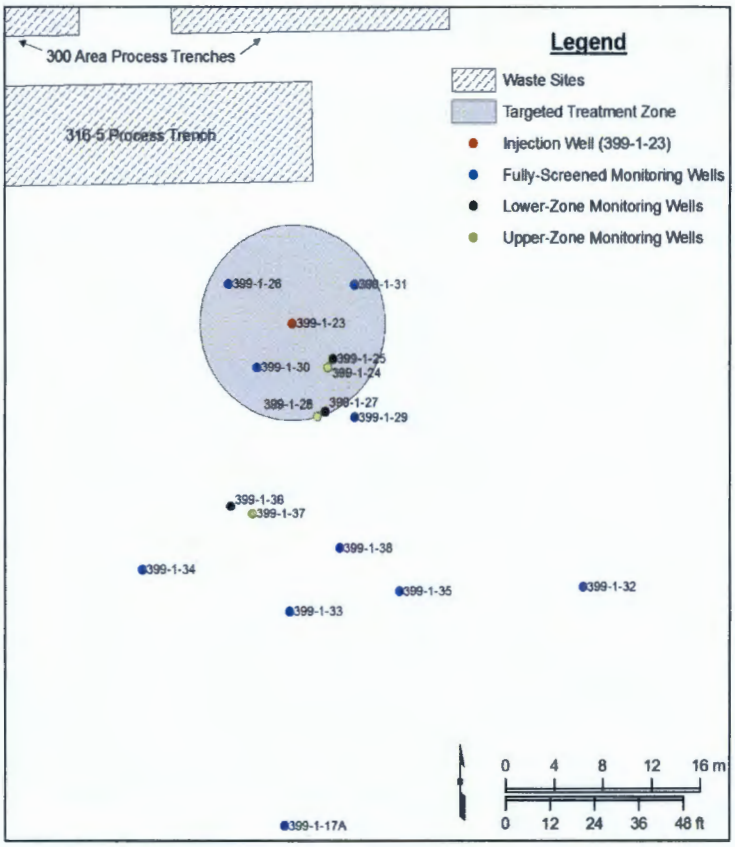

Figure 2.1. Polyphosphate Treatability Test Site Well Layout

Table 2.1. Pilot-Scale Field Test Amendment Formulation

Injection	Amendment	Formula	Formula Wt, g/mol	Solubility, g/L 23°C H_2O	Density, g/cm^3 (25°C)	Conc., g/L	Conc., M
1	Sodium phosphate, monobasic	NaH_2PO_4	119.98	29.63	1.004	0.59	4.94×10^{-3}
	Sodium pyrophosphate	$Na_4P_2O_7$	265.9	32.81		0.66	2.47×10^{-3}
	Sodium tripolyphosphate	$Na_5P_3O_{10}$	367.86	60.40		1.21	3.29×10^{-3}
	Sodium bromide	NaBr	102.90			0.103	1.00×10^{-3}
2	Calcium chloride	$CaCl_2$	110.98	800	1.005	3.41	3.07×10^{-2}
3	Sodium phosphate, monobasic	NaH_2PO_4	119.98	29.63	1.004	0.59	4.94×10^{-3}
	Sodium pyrophosphate	$Na_4P_2O_7$	265.9	32.81		0.66	2.47×10^{-3}
	Sodium tripolyphosphate	$Na_5P_3O_{10}$	367.86	60.40		1.21	3.29×10^{-3}
	Sodium bromide	NaBr	102.90			0.103	1.00×10^{-3}

Table 2.2. Transport Parameters Determined by Direct Measurement or from a Laboratory-Derived Breakthrough Curve on the <2-mm Sediment Fraction[a]

Amendment[b]	F (cm^3/hr)	ρ_b (g/cm^3)	θ	V_w (mL)	v (cm/hr)	t_o (V_w)	R	K_d (mL/g)
Sodium orthophosphate	30.37	1.478	0.386	20.89	16.01	11.22	5.54	1.19
Sodium pyrophosphate	41.93	1.444	0.385	20.33	22.18	15.90	7.61	1.76
Sodium tripolyphosphate	40.80	1.460	0.392	21.27	21.22	14.70	5.17	1.12
Calcium	31.41	1.478	0.386	20.89	16.57	11.95	14.14	3.44
Amendment (Table 1, injection 1), pH 7	30.61	1.444	0.385	20.33	16.19	12.26	5.83	1.29
Amendment (Table 1, injection 1), no pH Adjustment	30.88	1.460	0.392	21.27	16.05	11.82	5.23	1.13

(a) F = flow rate; ρ_b = bulk density; θ = average volumetric water content (standard deviation); V_w = average pore volume; v = average pore water velocity; t_o = step input; R = retardation factor; K_d = sediment water distribution coefficient based on R.
(b) Columns appeared saturated and had reached a stable water content.

These values were adjusted for field conditions assuming that retardation was due to the <2-mm fraction and that the <2-mm fraction composed ~10% of the total sediment matrix. The field K_d and retardation values were calculated using a porosity value of 0.2 and bulk density value of 2.19 g/cm^3, which were quantified within the limited field investigation (LFI) (Table 2.3) (Wellman et al. 2007). Sorption of phosphate and calcium to the sedimentary matrix is relatively slow, requiring several hours. Due to kinetic considerations, flow rates resulting in more rapid transport of calcium and phosphate within the sedimentary matrix will significantly reduce the retardation, resulting in less mixing of injection phases during remedy implementation.

Table 2.3. Field Transport Parameters Calculated from Laboratory-Derived Transport Parameters

Amendment	v (m/d)	R	K_d (mL/ g)
Sodium orthophosphate	16.21	2.30	0.12
Sodium pyrophosphate	22.82	2.93	0.18
Sodium tripolyphosphate	21.84	2.23	0.11
Calcium	17.26	4.76	0.34
Amendment, pH 7	17.60	2.41	0.13
Amendment, no pH Adj.	17.56	2.24	0.11

2.2 Low Surface Area

During the pilot-scale field test, limited mixing between the calcium and phosphate that were injected resulted from a combination of factors. These include, but are not limited to 1) the rate of injection used during remedy emplacement (756 L/min), 2) the groundwater velocity (15.24 m/day) within the 300 Area, 3) the open framework sedimentary matrix, which possesses minimal fine-textured particles, and 4) low effective retardation values for calcium and phosphate within the 300 Area subsurface. For example, Figure 2.2 is a graph of the normalized breakthrough curves (BTCs) for calcium, phosphate, chloride, and bromide at monitoring well 399-1-29. The results displayed in Figure 2.2 are representative of those observed at most wells within the field test site. The effective retardation of the first phosphate injection

was $R_{ef} = 0.35$, the effective retardation of the calcium injection was $R_{ef} = 0.58$, and the effective retardation of the second phosphate injection was $R_{ef} = 0.45$. The slightly higher effective retardation of the final phosphate injection suggests a slight overlap and mixing with the calcium injection. However, the effective retardation for the calcium and polyphosphate injections during the field test were significantly less than the retardation factors of $R_{ef} = 4.76$ and $R_{ef} = 2.41$ for calcium and the polyphosphate amendment, respectively. The limited retardation observed under field conditions limited the mixing of the three remedy phases. Furthermore, Wellman et al. (2007) previously noted that the ratio of calcium to phosphate needed to precipitate apatite is highly sensitive. The highly variable hydrodynamic conditions present in the 300 Area subsurface challenge the ability to control this variable. These factors limit the in situ formation of apatite to quantities that are less than the amount predicted based on the stoichiometry of the injection formulations.

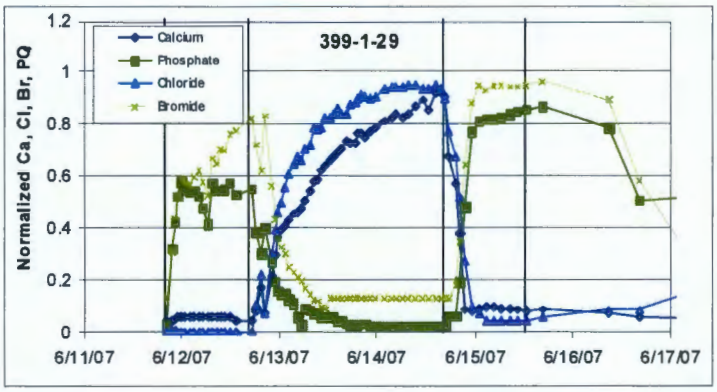

Figure 2.2. Normalized BTC for Calcium, Phosphorus, Chloride, and Bromide at Down-Gradient Well 399-1-29. the curve displays characteristic results with limited mixing of the calcium and phosphorus injections during the pilot-scale field test.

Although numerous bench-scale column experiments were conducted and an optimum formulation and the injection strategy was designed for implementation under pore water velocities of 15.24 m/day, the flow rates used for injection during the field-scale pilot test exceeded the conditions that were tested. As a result, the effective retardation of calcium and phosphorus were significantly reduced. This resulted in a limited amount of mixing between the amendment phases. Alternative injection strategies and amendment formulations could be designed to afford greater mixing by assuming limited retardation of both calcium and polyphosphate. These alternate strategies could consist of 1) significantly shorter injection durations for alternating pulses of calcium and polyphosphate, 2) a revised amendment formulation containing a higher content of ortho- and pyrophosphate which would increase reaction rates, and 3) investigation of possible inclusion of tripolyphosphate, or longer chains, within the calcium injection phase. Additional bench- and large-scale laboratory testing would be necessary to develop these alternate strategies.

2.3 High Solution-to-Apatite Ratio

Based on results obtained from the field tracer study, effective porosities were calculated for each of the eight monitoring wells in the targeted injection volume (Table 2.4). Values range from 11 to 32% for the different wells, with an average effective porosity of 19%. This value is consistent with porosity estimates from the LFI that were based on physical property analysis (Williams et al. 2007).

Table 2.4. Bromide Tracer Injection Arrival Times and Porosity Results for Targeted Injection Volume Monitoring Wells

Well Name	Well Screen Zone	Radial Distance (m)	50% Tracer Arrival (min)	Average Velocity (m/day)	Estimated Effective Porosity
399-1-23	Full	0	-	-	-
399-1-24	Upper	4.54	124	51.82	0.32
399-1-25	Lower	4.39	39	161.54	0.11
399-1-26	Full	6.07	111	79.25	0.16
399-1-27	Lower	7.47	428	N.C.	N.C.
399-1-28	Upper	7.59	216	51.8	0.20
399-1-29	Full	9.02	310	42.6	0.20
399-1-30	Full	4.51	16	N.C.	N.C.
399-1-31	Full	5.97	90	94.49	0.13
					Average = 0.19

N.C. = not calculated due to uncharacteristic response.

Based on the average effective porosity of 19% and a bulk density of 2.21 g/cm^3, the sediment-to-water ratio in the 300 Area is 12.28 g/cm^3. Thus, 1 cm^3 of aquifer has 0.8 cm^3 of sediment and 0.2 cm^3 of groundwater. Assuming quantitative precipitation of apatite was achieved during the pilot-scale field test, ~0.025 wt% of hydroxyapatite could have been precipitated. At 0.025 wt% apatite in the sediment, the solution-to-apatite ratio would be 325 mL/g apatite. Alternatively, achieving a maximum target wt% of 0.1 wt% apatite under field condition, 0.0008 g of apatite would have precipitated, thereby affording a solution-to apatite ratio of 81 to 1. Static laboratory tests were conducted to evaluate the efficacy of apatite for the sequestration of uranium as a function of the solution-to-solid ratio bracketing the range of attainable solution-to-solid ratios during remediation activities in the field. Figure 2.3 shows the results of laboratory batch tests conducted as a function of pH with an initial aqueous uranium concentration of 1 mg/L. The removal of uranium is invariant as a function of pH under the range of 6 to 7 and increases linearly over the solution-to-solid ratio of 0 to 1,000. Under these conditions, it was possible to sequester up to 100 mg U/g apatite. Between pH 7 and 8 the mass of uranium removed increases linearly up to the solution-to-solid ratio of 200. At solution-to-solid ratios >200 and pH 8, the mass of uranium removed from solution displays a gradual increase from ~30 mg U/ g apatite to a maximum of ~50 mg U/ g apatite. Thus, the potential efficiency for sequestration of uranium with apatite under conditions present within the 300 Area is within the range spanning the upper bounds between pH 7 and 8.

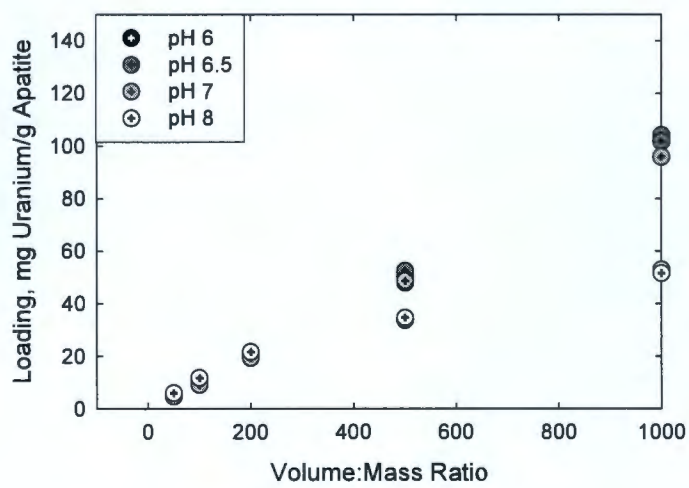

Figure 2.3. Uranium Loading (mg uranium/g hydroxyapatite) on Hydroxyapatite (as a function of the volume-to-mass ratio over the pH range of 6 to 8 in hydroxyapatite-equilibrated groundwater)

3.0 Effect of 300 Area Geochemical Conditions on the Removal and Long-Term Retention of Uranium with Apatite

Uranium chemistry is highly influenced by a number of geochemical variables, including pH and carbonate concentrations, which are particularly important. In addition, the long-term stability of uranium sequestered by apatite is dependent on the chemical speciation of uranium, the surface speciation of apatite, and the mechanism of retention, which is highly susceptible to dynamic geochemical conditions. Several bench-scale studies (described below) were performed to evaluate the effects of these two variables on the sequestration of uranium on apatite.

3.1 Effects of pH on Adsorption of Uranium on Apatite

Figure 3.1 displays historical pH values for a number of select near-river and inland wells near the 300 Area polyphosphate pilot test site. During the late 1980s and early 1990s, the pH of the groundwater within this region was strongly influenced by liquid waste disposal to process ponds and trenches. As such, the pH ranged from 6.7 to 8.0, with occasional spikes in pH being due to high river years and a reduction in the dilution from the cessation of disposal to the trenches. It was originally assumed that the groundwater pH would decrease in locations near the river, because of the effect of lower pH river water. However, as can be seen in Figure 3.1, that appears not to be the case. Over the past 10 years the groundwater pH has stabilized and is generally within the range of 7.5 to 8.0.

Kinetic sequestration experiments were conducted to evaluate the rate of uranium uptake in the presence of hydroxyapatite at a solution-to-apatite ratio of 325 mL/g apatite. Figure 3.2 shows the dependence of uranium uptake, expressed as aqueous uranium concentration, in the presence of hydroxyapatite under the pH range of 7 to 8. The rate of uranium removal from the aqueous phase was rapid and equilibrium was attained within the first minute of the reaction. In the presence of 120 μg/L aqueous uranium, 100% of the uranium was removed within the first minute. This reflects the abundance of available surface sites for sorption and/or surface complexation of uranium. These kinetic results do not show any apparent limitations to uranium removal via apatite sequestration under the pH range of 7 to 8. However, it must be noted that under the given conditions the amount of available surface sites exceeds the aqueous uranium concentration. During remediation activities, as more uranium enters the treatment zone, the conditions will shift from those in which the number of available surface sites exceeds the concentration of uranium to the alternative condition wherein, the concentration of uranium will exceed the available surface sites. Therefore, an additional set of static batch tests was conducted to evaluate the rate and extent of uranium sequestration with apatite under conditions where uranium exceeds the number of adsorption sites.

Figure 3.3 shows the dependence of uranium uptake expressed as aqueous uranium concentration in the presence of hydroxyapatite under the pH range of 6 to 8, 23°C, given an aqueous uranium concentration of 100 ppm and solution-to-solid ratio of 100 to 1. Compared to the results presented in Figure 3.2, the rate of uranium removal was still rapid over the pH range. At pH $\leq$7, 100% of the aqueous uranium was removed within the first 2 minutes. However, under the pH range of 7.5 to 8, only ~15% of the aqueous uranium was removed within the first 2 minutes. Subsequently, further removal of aqueous uranium was minimal. Thus, as the concentration of aqueous uranium increases within the treatment zone and more uranium is sequestered on the apatite surface, the rate and extent of uranium sequestration exhibits a greater dependence on pH and decreased performance at pH values $\geq$7.5.

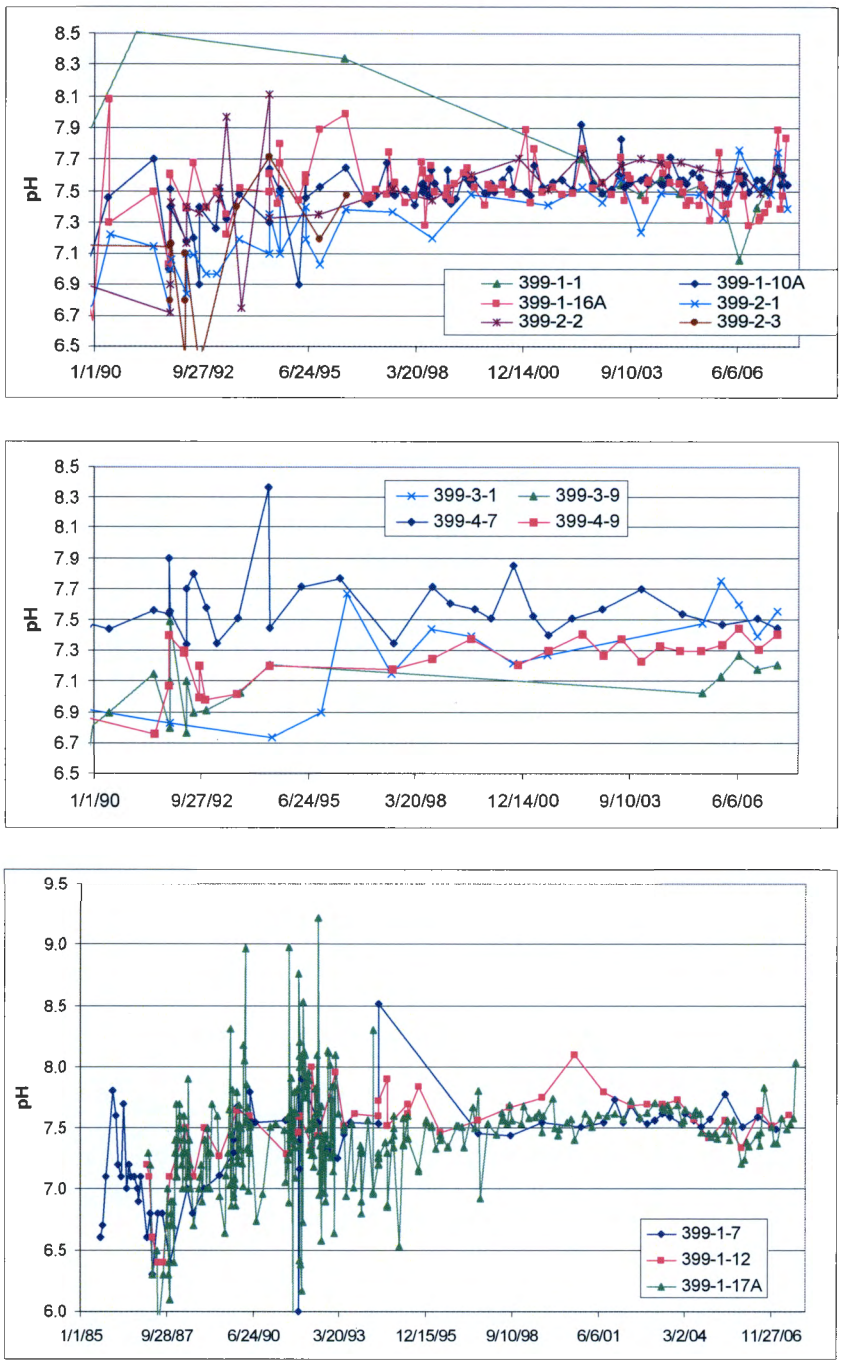

Figure 3.1. Historical pH Values of Selected Near-River and Inland Wells in the 300 Area

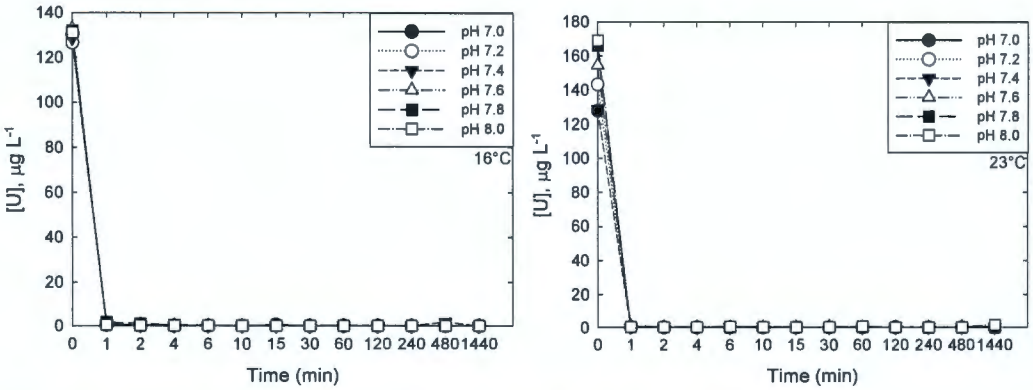

Figure 3.2. Dependence of Uranium Sequestration with Apatite Given a Solution-to-Solid Ratio of 325 mL/g Apatite. Uranium sequestration is expressed as aqueous uranium concentration versus time over the pH range of 7 to 8 in Hanford groundwater at 16° and 23°C.

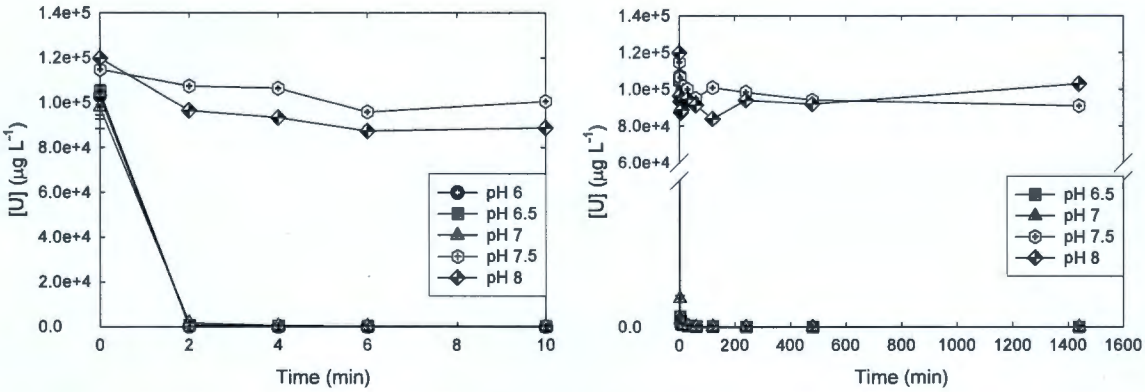

Figure 3.3. Dependence of Uranium Uptake Expressed as Aqueous Uranium Concentration as a Function of Time over the pH Range of 6 to 8 in Hydroxyapatite-Equilibrated Groundwater.

3.2 Effects of Speciation on the Sequestration of Uranium on Apatite

The pH and concentration of CO_2 impart a significant influence on the speciation of aqueous uranium and the reactive sites present on the surface of hydroxyapatite. Under the pH range of 6 to 8, the aqueous speciation of uranium changes from predominantly $UO_2(CO_3)_2^{4-}$ and $UO_2(CO_3)_2^{2-}$ to the more weakly charged species $Ca_2UO_2CO_3$ and $(UO_2)_2(CO_3)(OH)_3^-$. Additionally, hydroxyapatite surfaces are hypothesized to have two different types of surface groups: $\equiv$Ca-OH_2^+ and $\equiv$P-OH, affording a pH_{pzc} of 8.15 or 7.13 upon exposure to atmospheric CO_2 (Wu et al. 1991). Below a pH of 4, the phosphate sites are predicted to be fully protonated, $\equiv$P-OH. Above pH 4, the phosphate sites begin to deprotonate, thereby affording a fraction of $\equiv$P-OH and $\equiv$P-O^- sites, depending upon the pH. Near pH $\cong$ 6.6 the surface speciation is predicted to be approximately 50% $\equiv$P-OH and 50% $\equiv$P-O^-. At a pH of ~7, $\equiv$Ca-OH_2^+ surface sites begin to deprotonate, and at a pH $\cong$ 9.7 affords approximately 50% $\equiv$Ca-OH_2^+ and 50% $\equiv$Ca-OH (Wu et al. 1991). Integrating changes in both the aqueous speciation of uranium and the speciation of reactive surface sites on hydroxyapatite can result in significant variations in the efficacy and mechanism of hydroxyapatite for sequestration of uranium under the pH range encountered within the 300 Area aquifer, pH = 7 to 8. To evaluate the effects of these variables on uranium sequestration, static batch tests were conducted at a solution-to-solid ratio of 325 mL/g apatite in the presence of 120 µg/L

aqueous uranium at 16° and 23°C. These conditions are relevant to those that could have been encountered during the field-scale pilot test having precipitated 0.025 wt% apatite. Additionally, these conditions afford an excess of reactive surface sites to evaluate the subtle effects of pH and carbonate concentration on the sequestration of uranium on hydroxyapatite under a narrow pH range.

Figure 3.4 displays the equilibrium partition coefficients, K_d values, as a function of pH. Results presented here illustrate the sensitivity of aqueous uranium speciation and the speciation of reactive surface sites on the sequestration of uranium with apatite. At 23°C, the amount of uranium sequestered on apatite decreases sharply over the pH range of 7.0 to 7.4; under the pH range of 7.4 to 8.0, there is a slight increase in the sequestration of uranium. Comparatively, the apparent sequestration of uranium with apatite at 16°C displays noted differences relative to that observed at 23°C. First, under the pH range of 7.0 to 7.4 there is no decrease in uranium sequestration. From pH 7.4 to 8.0, K_d values at 16°C are approximately 4 times greater than those quantified at 23°C. Although there is a slight apparent increase in uranium sequestration over the pH range of 7.4 to 8.0, consideration of the error associated with these measurements indicates there is little difference in the amount of uranium sequestered over this pH range. The observed deviations in uranium sequestration can be explained, in part, by coupled changes in both the aqueous speciation of uranium, as well as the speciation of reactive surface sites, resulting from changes in pH and a reduction in pCO_2 with decreasing temperature.

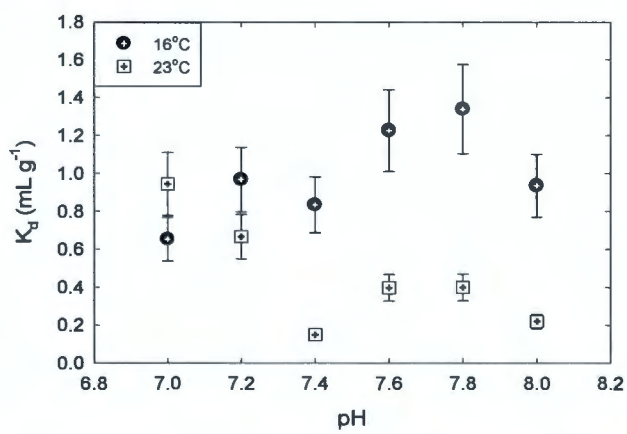

Figure 3.4. Equilibrium Distribution Coefficients for Uranium (VI) Sorption on Hydroxyapatite as a Function of pH

In addition to imparting significant influence on the aqueous speciation of uranium and the speciation of reactive surface sites, the high carbonate concentrations in the 300 Area subsurface also impact the mechanism of uranium retention with hydroxyapatite. Fuller et al. (2002) previously demonstrated that in the absence of carbonate, sorbed uranium concentrations in excess of 5500 μg U(VI) g^{-1} resulted in the precipitation of chernikovite (H-autunite). However in the presence of carbonate, chernikovite formation was not observed, even with uranium loadings up to 12,300 μg U(VI) g^{-1}. Thus, it is expected that sorption and/or surface complexation of uranium could occur until all surface sites have been depleted, but the high carbonate concentrations in the 300 Area would act to inhibit the transformation of sorbed uranium to chernikovite and/or autunite. Therefore, the efficacy of uranium retention of apatite will be governed by the rates of uranium desorption and phosphate release during apatite dissolution rather than conversion of sorbed uranium to autunite, or other stable uranium phases.

A series of static, sequential desorption tests was conducted to evaluate the rate of uranium desorption from hydroxyapatite under conditions relevant to remediation within the 300 Area aquifer. Figure 3.5 illustrates the release of uranium, measured in laboratory batch tests, based on the total amount of uranium removed, as a function of the cumulative volume of Hanford groundwater. The solution-to-apatite ratio was 100 to 1, which was equivalent to the maximum target wt% of 0.1% apatite in the field sediment. The release of uranium in Hanford groundwater matrices displayed a direct relationship with increasing pH. Under the pH range of 6 to 7, the uranium was tightly retained with apatite after contact with ~40 mL of fresh groundwater, equivalent to approximately 4000 pore volumes. Under the pH range of 7.5 to 8, the release of uranium from apatite displayed a rapid linear increase in the amount of uranium released from apatite with increasing volumes of fresh groundwater. After ~40 mL of fresh groundwater, ~0.5 % of the sorbed uranium was released.

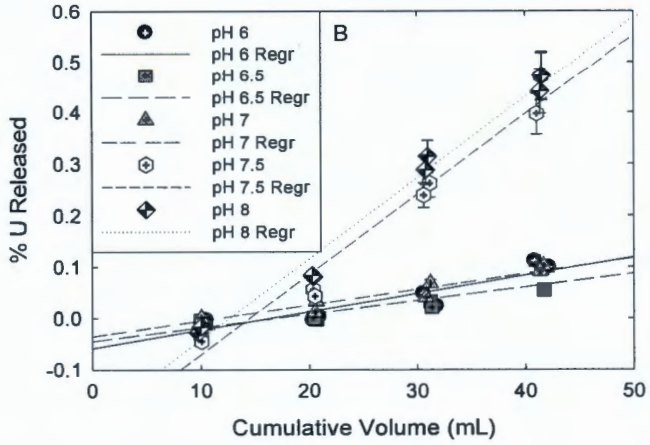

Figure 3.5. Percent Release of Uranyl from Hydroxyapatite as a Function of the Cumulative Volume of Hanford Groundwater.

4.0 Summary

Two separate overarching issues affect the efficacy of apatite remediation for uranium sequestration within the 300 Area: 1) the efficacy of apatite for sequestering uranium under the present geochemical and hydrodynamic conditions, and 2) the formation and emplacement of apatite via polyphosphate technology. In addition, the long-term stability of uranium sequestered via apatite is dependent on the chemical speciation of uranium, surface speciation of apatite, and the mechanism of retention, which is highly susceptible to dynamic geochemical conditions. It is expected that uranium sequestration in the presence of hydroxyapatite would occur by sorption and/or surface complexation until all surface sites have been depleted, but the high carbonate concentrations in the 300 Area would act to inhibit the transformation of sorbed uranium to chernikovite and/or autunite. Adsorption of uranium by apatite was never considered a viable approach for in situ of uranium sequestration in of itself, because by definition, this is a reversible reaction. The efficacy of uranium sequestration by apatite assumes that the adsorbed uranium would subsequently convert to autunite, or other stable uranium phases. Because this appears to not be the case in the 300 Area aquifer, even in locations near the river, apatite may have limited efficacy for the retention and long-term immobilization of uranium at the 300 Area site.

5.0 References

Fuller CC, JR Bargar, JA Davis, and MJ Piana. 2002. "Mechanisms of Uranium Interactions with Hydroxyapatite: Implication for Groundwater Remediation." *Environmental Science and Technology* **36**:158-165.

Wellman DM, EM Pierce, EL Richards, BC Butler, KE Parker, JN Glovack, SD Burton, SR Baum, ET Clayton, and EA Rodriguez. 2007. *Interim Report: Uranium Stabilization through Polyphosphate Injection – 300 Area Uranium Plume Treatability Demonstration Project*, PNNL-16683, Pacific Northwest National Laboratory, Richland, Washington.

Williams BA, CF Brown, W Um, MJ Nimmons, RE Peterson, BN Bjornstad, RJ Serne, FA Spane, and ML Rockhold. 2007. *Limited Field Investigation Report for Uranium Contamination in the 300 Area, 300-Ff-5 Operable Unit, Hanford Site, Washington*, PNNL-16435, Pacific Northwest National Laboratory, Richland, Washington.

Wu L, W Forsling, and PW Schindler. 1991. "Surface Complexation of Calcium Minerals in Aqueous Solution 1. Surface Protonation a Fluorapatite-Water Interfaces." *Journal of Colloid and Interface Science* **147**(178).

Distribution

No. of Copies		
1	**DOE-Richland Operations Office**	
	K. M. Thompson	A6-38

No. of Copies		
5	**Pacific Northwest National Laboratory**	
	J. S. Fruchter	K6-96
	V. R. Vermeul	K6-96
	D. M. Wellman	K3-62
	E. M. Pierce	K3-62
	M. D. Williams	K6-96